Molecular Plant Pathology

MOLECULAR PLANT PATHOLOGY (2018) 19(7), 1765–1778 DOI: 10.1111/mpp.12659

The common bean COK-4 and the Arabidopsis FER kinase domain share similar functions in plant growth and defence

RAFHAEL FELIPIN AZEVEDO [1,2], MARIA CELESTE GONÇALVES-VIDIGAL [2], PAULA RODRIGUES OBLESSUC [1,*] AND MAELI MELOTTO [1,*]

[1]Department of Plant Sciences, University of California, Davis, Davis, CA 95616, USA
[2]Departamento de Agronomia, Universidade Estadual de Maringá, Maringá, PR 87020-900, Brazil

SUMMARY

Receptor-like kinases are membrane proteins that can be shared by diverse signalling pathways. Among them, the *Arabidopsis thaliana* FERONIA (FER) plays a role in the balance between distinct signals to control growth and defence. We have found that COK-4, a putative kinase encoded in the common bean anthracnose resistance locus *Co-4*, which is transcriptionally regulated during the immune response, is highly similar to the kinase domain of FER. To assess whether COK-4 is a functional orthologue of FER, we expressed *COK-4* in the wild-type Col-0 and the *fer-5* mutant of Arabidopsis and evaluated FER-associated traits. We observed that *fer-5* plants show an enhanced apoplastic and stomatal defence against *Pseudomonas syringae*. In addition, the *fer-5* mutant shows reduced biomass, smaller guard cell size, greater number of stomata per leaf area, fewer leaves, faster transition to reproductive stage and lower seed weight per plant than the wild-type Col-0. Except for the stomatal complex length and number of stomata, *COK-4* expression in *fer-5* lines partially or completely rescued both defence and developmental defects of *fer-5* to the wild-type level. Notably, COK-4 may have an additive effect to FER, as the expression of *COK-4* in Col-0 resulted in enhanced defence and growth phenotypes in comparison with wild-type Col-0 plants. Altogether, these findings indicate that the common bean COK-4 shares at least some of the multiple functions of the Arabidopsis FER kinase domain, acting in both the induction of plant growth and regulation of plant defence.

Keywords: *Arabidopsis thaliana*, *Co-4* locus, FERONIA, *Phaseolus vulgaris*, plant growth and development, plant immunity.

INTRODUCTION

In order to resist pathogen invasion, plants induce innate immune responses that are often associated with a reduction in plant growth (Campos *et al.*, 2016; Lozano-Durán and Zipfel, 2015). This plant growth–defence balance is regulated by a crosstalk between different hormones and depends on both physiological and environmental factors (Huot *et al.*, 2014; Züst and Agrawal, 2017). Pattern recognition receptors (PRRs) are often receptor-like kinases (RLKs) that are important in self- and non-self-recognition. Some PRRs can be shared by different signalling pathways and work to fine tune plant responses to endogenous and exogenous stimuli; thus, PRRs play an important role in the regulation of growth–defence tradeoffs in plants (Belkhadir *et al.*, 2014).

Amongst the subfamilies of RLKs, members of the *Catharanthus roseus* RLK1-like (CrRLK1L) subfamily are known to be growth controlling elements (Nissen *et al.*, 2016). FERONIA (FER), a member of the CrRLK1L subfamily in *Arabidopsis thaliana* (L. Heyhn.), is involved in pollen tube perception in the megagametophyte (Escobar-Restrepo *et al.*, 2007) and is a key regulator of cell expansion during vegetative growth (Guo *et al.*, 2009). In roots, FER acts as a receptor for the secreted hormone peptide RALF1 (rapid alkalinization factor 1) and controls cell expansion (Haruta *et al.*, 2014). In addition, FER can function in the crosstalk between plant hormones to regulate shoot growth. Brassinosteroid (BR) and ethylene signalling interact to balance hypocotyl growth through FER (Deslauriers and Larsen, 2010), whereas the crosstalk between abscisic acid (ABA) and auxin that enables normal shoot growth has FER as a convergent mediator (Yu *et al.*, 2012).

Interestingly, Kessler *et al.* (2010) reported that a homozygous *fer* mutant is resistant to powdery mildew infection, and shows spontaneous cell death and high H_2O_2 production; thus, FER has been linked to plant defence responses. In addition, Keinath *et al.* (2010) observed enhanced accumulation of reactive oxygen species (ROS) in *fer* mutants, as well as enhanced flg22-induced activation of mitogen-activated protein kinases (MAPKs), constitutively closed stomata and low proliferation of the ΔavrPtoΔavrPtoB mutant strain of the bacterial pathogen *Pseudomonas syringae* pv. *tomato* (*Pst*) DC3000, when compared with wild-type plants. More recently, FER has been implicated in susceptibility to *Fusarium oxysporum* by recognizing a fungus-produced RALF-like molecule, which acts as a virulence factor that inhibits host immune responses (Masachis *et al.*, 2016). Indeed, another Arabidopsis RALF peptide, RALF23, can dampen plant immune responses by recruiting FER and inhibiting the formation of the FLAGELLIN SENSING 2-BRASSINOSTEROID INSENSITIVE

*Correspondence: Email: problessuc@ucdavis.edu, melotto@ucdavis.edu

1/EF-TU RECEPTOR-ASSOCIATED KINASE (FLS2/EFR-BAK1) immune complex (Stegmann *et al.*, 2017).

We have found that COK-4, a putative serine/threonine (Ser/Thr) kinase encoded within the anthracnose-resistant locus *Co-4* from common bean (Melotto *et al.*, 2004), is highly similar to members of the CrRLK1L family of proteins from various species, including the Arabidopsis FER and ANXUR (Oblessuc *et al.*, 2015). Therefore, using genetic, physiological, phenotypic, molecular and *in silico* analyses, we sought to further understand the function of COK-4. We first identified *FER* (At3g51550) as a putative orthologue of *COK-4* in Arabidopsis and genetically complemented the Arabidopsis *fer-5* mutant, as well as transformed Col-0 control plants, with a *COK-4* open reading frame isolated from the common bean genotype G2333. We evaluated immune and growth responses in *COK-4*-expressing Arabidopsis lines. The results suggest that the kinase domain of FER shares similar functions to COK-4, where both may act as negative regulators of immunity against *Pst* DC3000 and may be involved in the positive regulation of plant growth and development.

RESULTS

COK-4 is closely related to the CrRLK1L family in Arabidopsis

Previously, we have identified COK-4 as being related to the kinase domain of protein members of the CrRLK1L family from various species (Oblessuc *et al.*, 2015). In order to characterize the COK-4 molecular function further, we searched the Arabidopsis genome for kinases that were most closely related to COK-4. Phylogenetic analysis revealed that COK-4 clusters with 15 of the 17 members of the CrRLK1L family in Arabidopsis (Fig. 1A). Amongst these CrRLK1L members, the kinase domain of FER showed the highest similarity to the whole COK-4 protein, with 38% sequence identity based on protein sequence alignment analysis (Fig. S1A, see Supporting Information). No sequence matches were observed between COK-4 and any other domain of all proteins used to create the phylogenetic tree (Figs S1A and S2, see Supporting Information). In addition, COK-4 shares serine, threonine and tyrosine residues with FER in phosphorylation sites that were identified by both software prediction and experimental analyses (Fig. S1A). However, FER seems to contain more phosphorylation sites than COK-4 (Fig. S1B). In addition, three-dimensional (3D) protein structure modelling for both COK-4 and FER proteins revealed that they share highly similar kinase domain structures (Fig. 1B). The hydrophobic domain (amino acids GSRFMSKQKQINVIVFWVIFVLLYELTHCH) of COK-4 contains the previously predicted transmembrane region (Melotto and Kelly, 2001) and, interestingly, this region is not present in the FER kinase protein (Figs 1B and S1A).

FER and other members of the CrRLK1L family have similar kinase domains to each other, as well as to COK-4 (Fig. S2; Kessler *et al.*, 2014). Therefore, to further confirm that FER was the best candidate for having similar functions to COK-4, we analysed the expression patterns of *FER* and the next two closest relatives of *COK-4*, *ANX1* and *ANX2*, based on protein phylogeny (Fig. 1A). Arabidopsis *ANX1* and *ANX2* are highly expressed, but not exclusively (Mang *et al.*, 2017), in mature pollen, whereas *FER* shows ubiquitous expression across all plant tissues (Fig. S3A–C, see Supporting Information). Furthermore, in our experimental conditions, the knockout mutants *anx1-1* and *anx2-2* (Boisson-Dernier *et al.*, 2009) have the same reaction to dip inoculation of *Pst* DC3000 as the wild-type Col-0 plants (Fig. S3D,E). In addition, it is important to highlight that FER is the CrRLK1L member of Arabidopsis that has a more comprehensive description of its function in plant immunity (Keinath *et al.*, 2010; Kessler *et al.*, 2010; Masachis *et al.*, 2016; Stegmann *et al.*, 2017). Thus, based on phylogeny, phosphorylation sites, 3D protein modelling analyses and its function on the plant immune response, FER was selected to facilitate the functional analysis of COK-4.

A functional FER contributes to stomatal opening and Arabidopsis susceptibility to *Pst* DC3000

In order to study the molecular function of COK-4, we first assessed the immune response phenotypes associated with FER mutation using the knockdown *fer-5* mutant (Fig. S4A,B, see Supporting Information). Duan *et al.* (2010) first described this mutant as having shoot and root growth deficiencies. Here, we observed that *fer-5* has a constitutively smaller stomatal aperture width when compared with Col-0 (Fig. 2A). When exposed to *Pst* DC3000, the *fer-5* stomatal aperture width decreases further within 2 h post-inoculation (hpi) (Fig. 2B), indicating that stomatal defence is active in *fer-5*. Interestingly, unlike Col-0, *fer-5* stomata do not respond to coronatine produced by this bacterium and remain closed at 4 hpi (Fig. 2B).

Pathogenesis assays revealed that *fer-5* shows increased resistance to *Pst* DC3000 independent of the inoculation method. Either surface inoculation or vacuum infiltration of bacteria into the apoplast resulted in significantly smaller bacterial populations within *fer-5* leaves relative to Col-0, as early as 1 day after inoculation (Fig. 2C,D). Furthermore, *fer-5* leaves showed no disease symptoms, whereas Col-0 leaves showed chlorotic and necrotic spots as expected for this pathosystem (Fig. 2C,D). These results suggest that the FER kinase is required for plant susceptibility to *Pst* DC3000, as *fer-5* shows enhanced stomatal and apoplastic defences.

COK-4 restores stomatal response and susceptibility to *Pst* DC3000 in *fer-5*

We observed that *fer-5* stomata do not re-open in response to *Pst* DC3000 and this plant is more resistant to bacterial infection (Fig. 2). Thus, we reasoned that these *fer-5* phenotypes could be

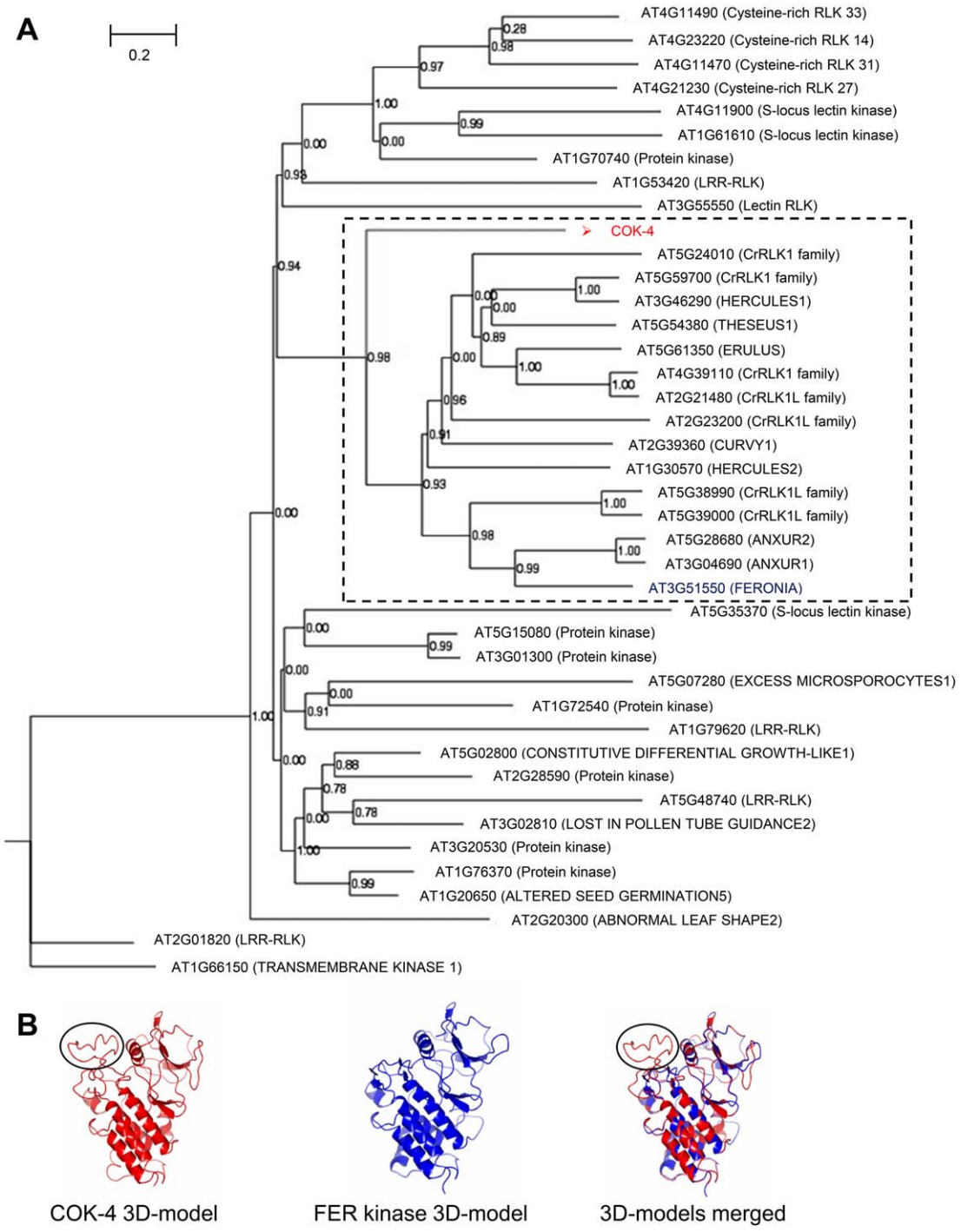

Fig. 1 COK-4 is highly similar to the Arabidopsis FERONIA (FER) kinase domain. (A) Phylogenetic tree showing the clustering of the predicted COK-4 protein with 15 of the 17 *Catharanthus roseus* RLK1-like (CrRLK1L) family members of Arabidopsis (broken square). The phylogenetic tree was obtained using the top 40 different protein kinases of Arabidopsis with significant alignment (threshold E-value $\leq 3 \times 10^{-33}$) with the predicted COK-4 protein from the common bean line SEL 1308 [National Center for Biotechnology Information (NCBI) accession number AAF98554; Melotto and Kelly, 2001], using the maximum parsimony method from MAFFT software (Katoh and Standley, 2013). The nodes were confirmed by 1000 bootstraps. (B) Three-dimensional (3D) protein structure of FER and COK-4 kinase domains showing that both kinases have similar structures. The protein models were obtained with SWISS-MODEL (https://swissmodel.expasy.org) and the alignment of the models was made using CCP4G v.2.10.6 (McNicholas *et al.*, 2011). The black circles indicate the COK-4 protein region that does not fit within the FER kinase domain structure. This region contains the transmembrane region of COK-4 predicted by Melotto and Kelly (2001). LRR, leucine-rich repeat; RLK, receptor-like kinase.

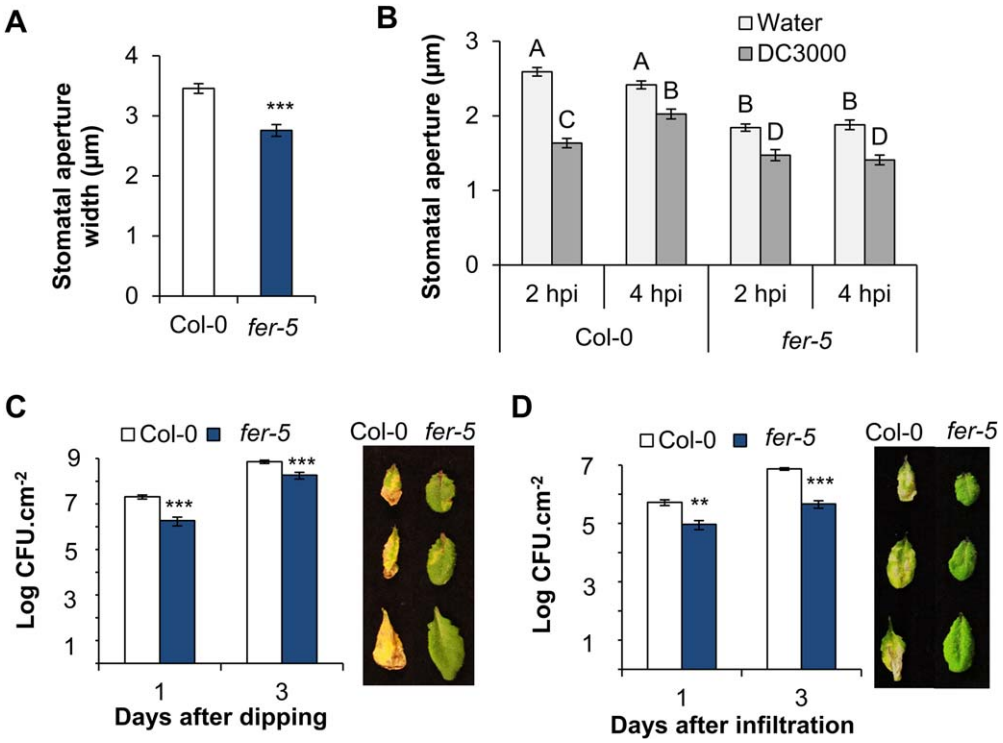

Fig. 2 A functional FERONIA (FER) kinase domain contributes to stomatal opening and Arabidopsis susceptibility to *Pseudomonas syringae* pv. *tomato* (*Pst*) DC3000. (A) Stomatal aperture width in untreated Col-0 and *fer-5* mature leaves. Results are shown as the mean ($n = 120 \pm$ SE) and statistical significance between the means was calculated with Student's *t*-test (***$P \leq 0.001$). (B) Stomatal aperture width in leaves inoculated with *Pst* DC3000 [1×10^8 colony-forming units (CFU)/mL] at two time points: 2 and 4 h post-inoculation (hpi). Results are shown as the mean ($120 < n < 180 \pm$ SE) and statistical significance amongst the means, indicated by different letters above the bars, was calculated with analysis of variance (ANOVA) followed by Scott–Knott's test ($P \leq 0.05$). (C, D) Apoplastic bacterial population in leaves after dip inoculation with 1×10^8 CFU/mL (C) or vacuum infiltration with 1×10^6 CFU/mL (D) of *Pst* DC3000, 1 and 3 days after inoculation. Results are shown as the mean ($n = 6 \pm$ SE) (Student's *t*-test; ***$p \leq 0.001$ and **$p \leq 0.01$). Photographs on the right were taken from various leaves at 3 days post-inoculation.

complemented by expressing a kinase closely related to the FER kinase domain, such as COK-4. To test this possibility, we first created two lines of Col-0 and *fer-5* expressing the p35S-*GFP*::*COK-4* construct (Col-0/*GFP*::*COK-4* lines 8 and 14, and *fer-5*/*GFP*::*COK-4* lines 10 and 12), as well as the empty vector as controls (Col-0/*GFP* and *fer-5*/*GFP*). Transient expression of these constructs in *Nicotiana benthamiana*, followed by western blot analysis, confirmed that the proteins were being expressed at the expected size (Fig. S5A, see Supporting Information). These constructs were then used to create stable Arabidopsis transgenic lines. Plant transformation was confirmed by imaging under fluorescence microscopy, and two independent transgenic lines for each construct were selected for further experimentation (Fig. 3).

Col-0 and *fer-5* plants expressing the green fluorescent protein gene (*GFP*) have the same stomatal response to *Pst* DC3000 as non-transformed plants (Fig. S5B,C), and the expression of COK-4 in both genetic backgrounds does not interfere with stomatal defence (i.e. the stomatal pores still close at 2 hpi) (Fig. 4A). Interestingly, expression of COK-4 in *fer-5* plants restored the

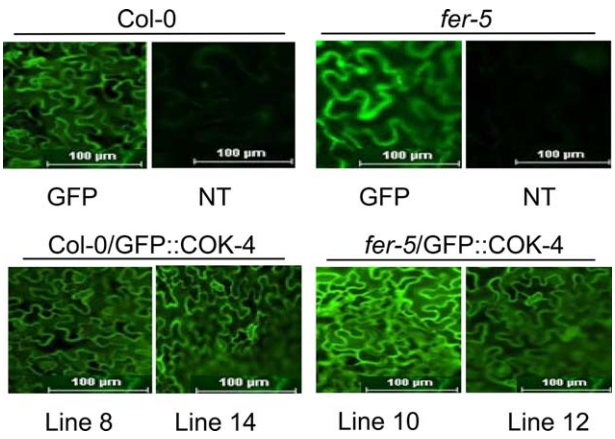

Fig. 3 Transgenic lines expressing constructs driven by the 35S promoter. Fluorescence micrographs of Col-0 and *fer-5* Arabidopsis leaves expressing either the green fluorescent protein gene (*GFP*) or the *GFP*::*COK-4* construct, as well as non-transformed (NT) Col-0 and *fer-5* leaves as a negative control. Two independent transgenic lines expressing *GFP*::*COK-4* were selected for further experimentation.

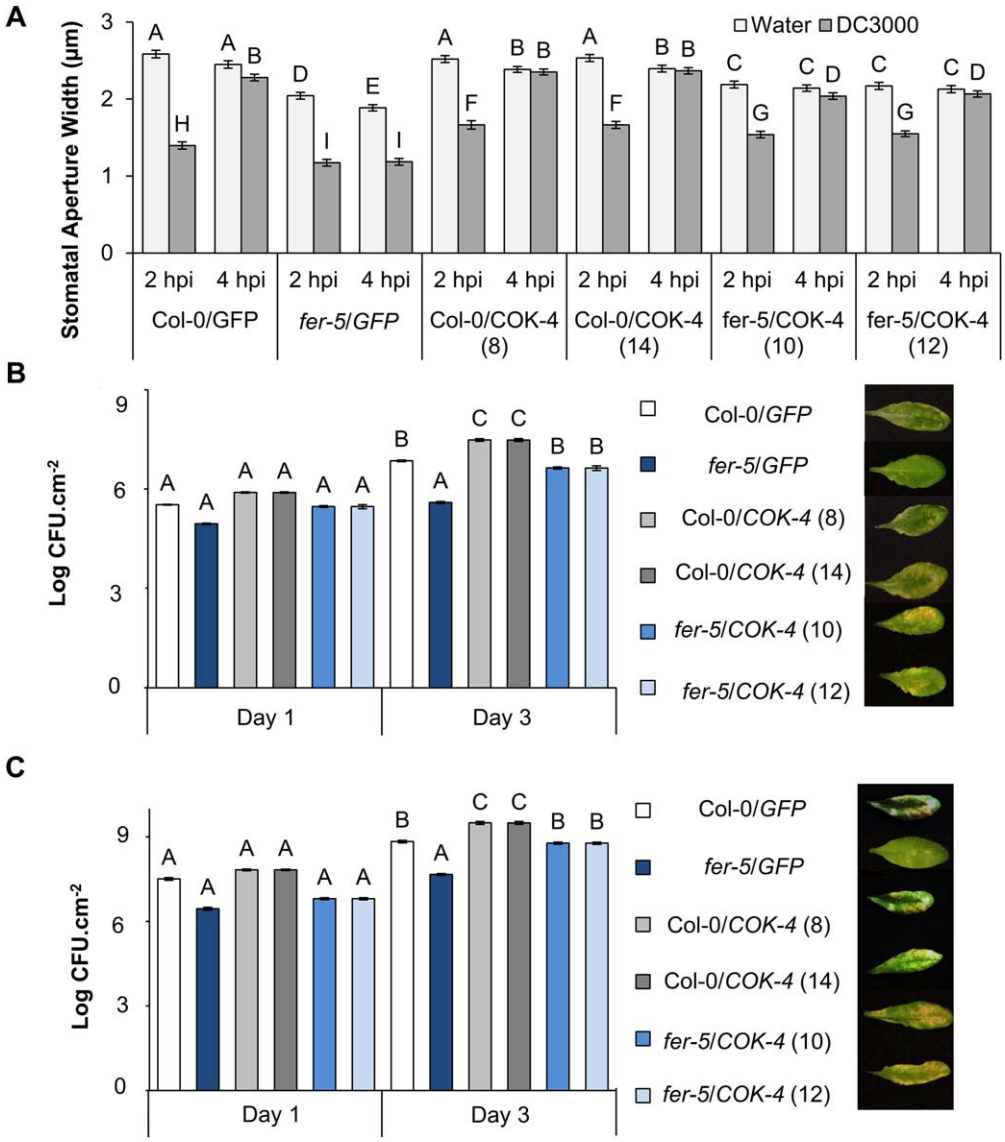

Fig. 4 *COK-4* expression increases susceptibility to *Pseudomonas syringae* pv. *tomato* (*Pst*) DC3000. (A) Stomatal aperture width at 2 and 4 h post-inoculation (hpi) with *Pst* DC3000 (1×10^8 CFU/mL). Results are shown as the mean ($n = 240 \pm$ SE). (B, C) Apoplastic bacterial population in leaves 1 and 3 days after dip inoculation with 1×10^8 CFU/mL (B) or vacuum infiltration with 1×10^6 CFU/mL (C) of *Pst* DC3000. Results are shown as the mean ($n = 18 \pm$ SE), and the statistical significance among the means, indicated by different letters above the bars, was calculated with analysis of variance (ANOVA) followed by Scott–Knott's test ($P \leq 0.05$). It should be noted that some error bars are too small to appear at the graph scale. Photographs on the right were taken from various leaves at 3 days post-inoculation.

wild-type stomatal response to *Pst* DC3000 and the stomatal pore re-opened at 4 hpi in these transgenic plants (Fig. 4A). In addition, *COK-4*-expressing Col-0 and *fer-5* lines supported increased bacterial apoplastic populations independent of the method of inoculation (dipping or vacuum infiltration) relative to the respective background plants expressing only *GFP* (Fig. 4B,C). Furthermore, *fer-5* lines expressing *COK-4* showed more severe symptoms in their leaves than in *fer-5*/*GFP* (Fig. 4B,C). Altogether, these results suggest that the bean COK-4 is a negative regulator of immunity and shares downstream partners in the same signalling pathway as the FER kinase during its action in plant defences against a bacterial pathogen.

COK-4 complements some of the *fer-5* growth and development defects

fer-5 stomata have constitutively smaller aperture widths than Col-0 stomata (Fig. 2A), which prompted us to take other measures of the stomatal complex to determine whether FER interferes with stomatal development. We found that, in addition to the

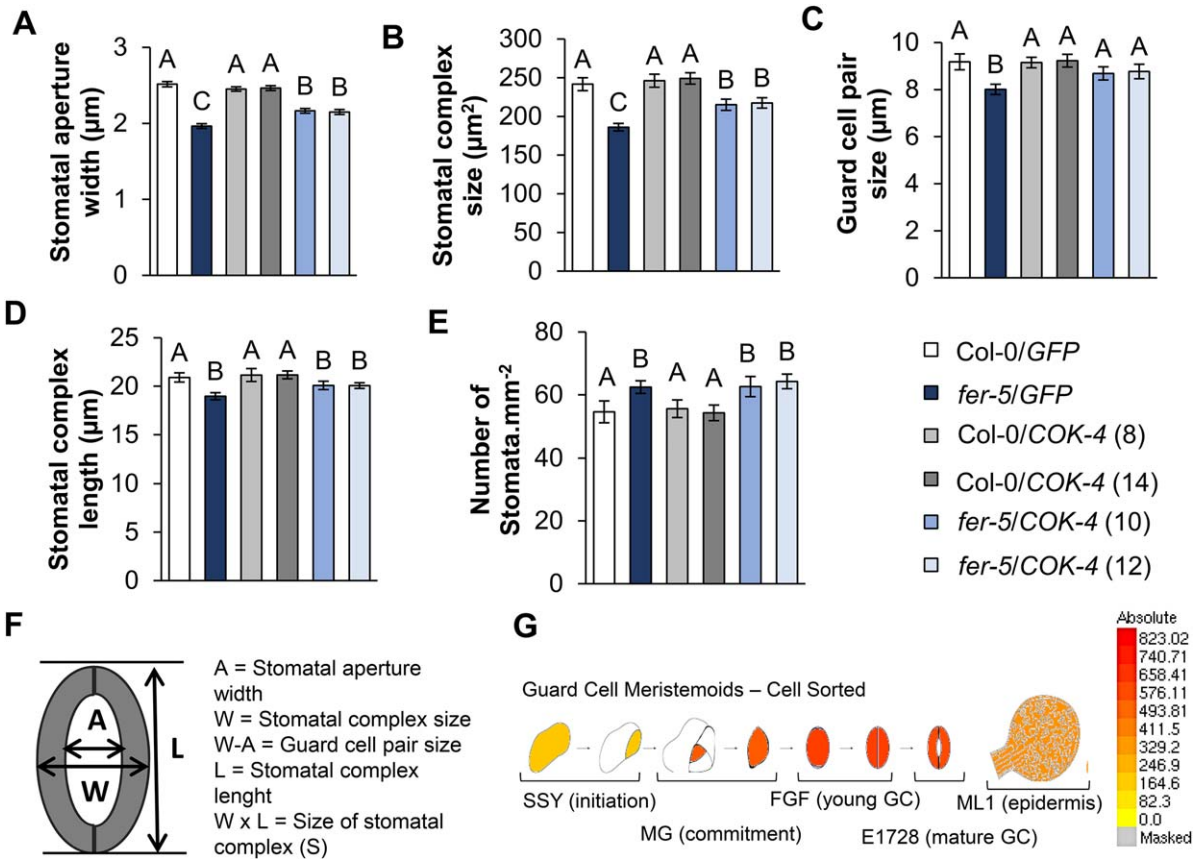

Fig. 5 COK-4 is required for normal stomatal development. Measurements were taken at 3 h after the lights were turned on in the morning: (A) stomatal aperture width; (B) stomatal complex size; (C) guard cell pair size; (D) stomatal complex length; (E) number of stomata per leaf area. Results are shown as the mean (n = 540 to 61 ± SE), and statistical significance amongst the means, indicated by different letters above the bars, was calculated with analysis of variance (ANOVA) followed by Scott–Knott's test ($P \leq 0.05$). (F) Diagram representing the measurements taken from stoma-forming guard cells. (G) Schematic representation of *FERONIA* (*FER*) gene expression during guard cell development in Arabidopsis adapted from eFBrowser.

stomatal aperture width, the stomatal complex size, guard cell pair size and stomatal complex length in *fer-5* are also smaller than in the wild-type plant (Fig. 5A–D). However, the *fer-5* mutant has a greater number of stomata per leaf area than Col-0 (Fig. 5E). Interestingly, expression of the COK-4 protein in the *fer-5* background partially rescued the stomatal width and stomatal complex size phenotypes, as indicated by ANOVA (Fig. 5A,B), and fully complemented the guard cell pair size (Fig. 5C). However, *COK-4* expression did not restore the stomatal complex length and number of stomata per leaf area (Fig. 5D,E). Expression of *COK-4* in Col-0 plants did not result in altered phenotypes relative to Col-0/*GFP* plants (Fig. 5A–E). Finally, the expression of *FER* increases during guard cell development, where mature guard cells express 1.9-fold more *FER* than stomatal lineage cells (Arabidopsis eFBrowser) (Fig. 5G). These results suggest that FER functions in stomatal development and that some aspects of this function are impacted by COK-4.

We also noticed that *fer-5* rosettes are smaller overall than those of Col-0 under the growth conditions set for the experiments (Fig. S6A, see Supporting Information; Duan *et al.*, 2010). Thus, a series of measurements was undertaken in order to quantify this phenotypic difference. We verified significant differences in fresh and dry weights, number of leaves at maturity (4–5 weeks of age), days to bolting and seed weight between the *fer-5* mutant and Col-0; however, no difference was observed in the number of days to emergence (Fig. S6B–G).

Next, we determined whether COK-4 could alter Col-0 growth and development, as well as complement the phenotypic defects of *fer-5* plants. Interestingly, Col-0/*COK-4* lines showed enhanced growth, i.e. higher rosette fresh and dry weights and more leaves, than Col-0/*GFP* (Fig. 6A–C), whereas Col-0/*GFP* and Col-0/*COK-4* showed the same average time to bolting and seed weight (Fig. 6D,E). Interestingly, *fer-5*/*COK-4* plants showed higher average values for all phenotypes

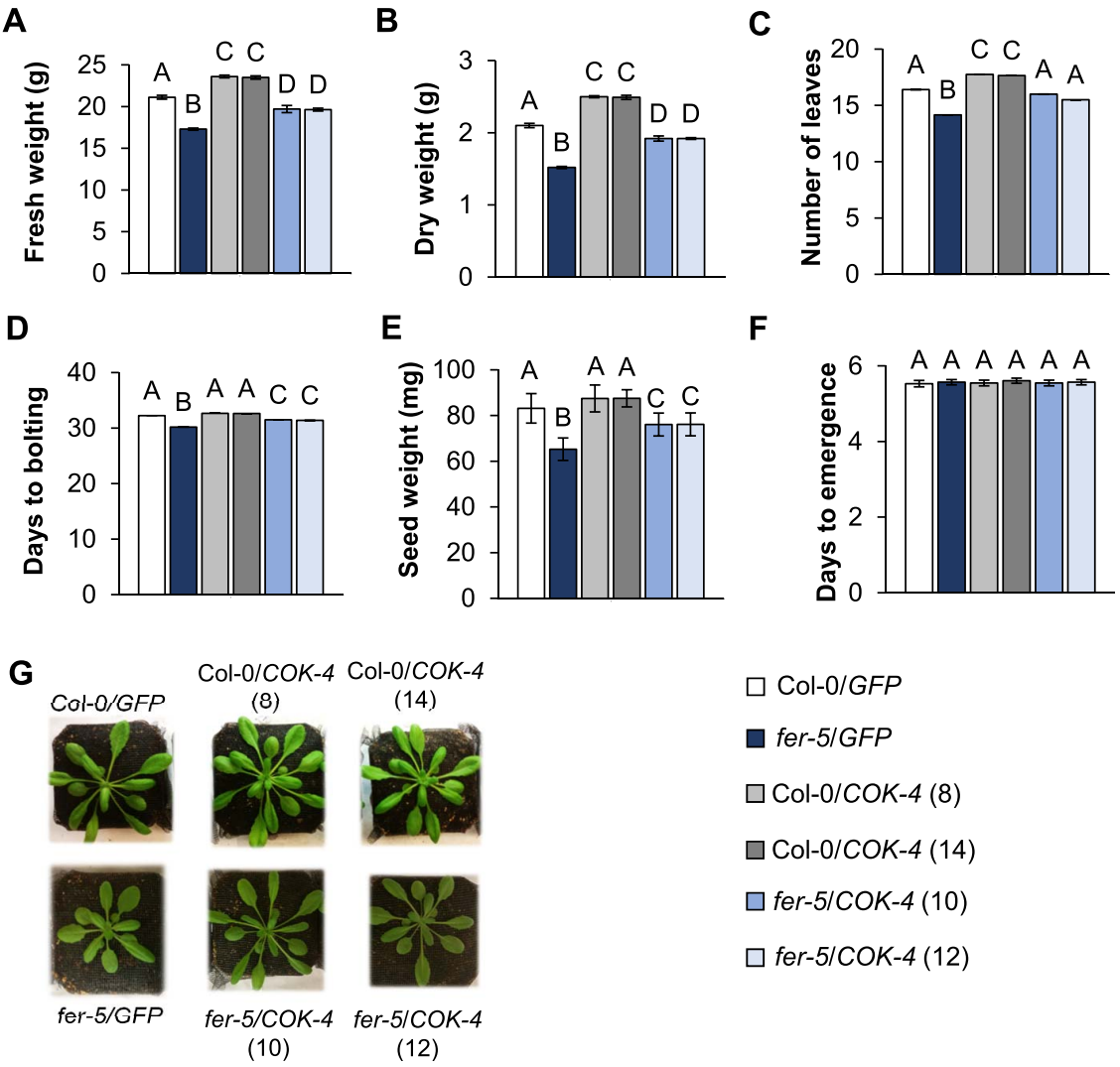

Fig. 6 COK-4 induces some aspects of plant growth and development. The graphs show the average fresh and dry weights of 4–5-week-old Arabidopsis rosettes ($n = 30 \pm$ SE) (A, B), number of leaves at maturity (4–5-week-old plants) ($n = 20 \pm$ SE) (C), days to bolting ($n = 28 \pm$ SE) (D), seed weight per plant ($n = 5 \pm$ SE) (E) and days to seedling emergence ($n = 51 \pm$ SE) (F). Statistical significance among the means, indicated by different letters above the bars, was calculated with analysis of variance (ANOVA) followed by Scott–Knott's test ($P \leq 0.05$). (G) Representative photographs of 4–5-week-old plants used for each measurement. Note that error bars in (C) and (D) are too small to appear in the graphs.

evaluated relative to *fer-5*/*GFP* plants (Fig. 6A–E). However, although COK-4 fully restored the number of leaves in the *fer-5* background (Fig. 6C), it partially rescued fresh and dry weights, days to bolting and seed weight (Fig. 6A,B,D,E). The number of days from sowing to seedling emergence did not change amongst the plant genotypes (Fig. 6F). The expression of *GFP* in *fer-5* and Col-0 plants did not affect the overall appearance of the rosettes relative to those of non-transformed plants, but an increase in rosette size was visible in *COK-4*-expressing lines (Fig. 6G). These findings suggest that the common bean COK-4 is an up-regulator of plant growth and functions in the same pathway as the Arabidopsis FER in controlling at least some aspects of plant growth and development.

DISCUSSION

We have previously described the *COK-4* gene from *Phaseolus vulgaris* as a promising source of plant defence against a broad range of pathogens. For instance, the bacterium *P. syringae* pv. *phaseolicola*, the causal agent of halo blight disease in beans, down-regulates a *COK-4-like* gene in an incompatible interaction with common bean (i.e. resistance), whereas the bacterial elicitor flagellin induces the expression of this gene (Oblessuc *et al.*,

2015). In this study, we used the model plant Arabidopsis to further characterize the role of COK-4 in plant immunity. We identified FER kinase as a putative orthologue of COK-4 in Arabidopsis by protein alignment and 3D structure modelling analyses (Fig. 1). FER was first described as being responsible for pollen tube recognition during pollination (Escobar-Restrepo *et al.*, 2007). Its partners in this process are two ANXUR proteins (ANX1/2) which contribute to the growth of the pollen tube (Miyazaki *et al.*, 2009). Although FER and ANX1/2 are closely related to each other and to COK-4 (Figs 1 and S2), unlike ANX1/2, FER is highly expressed in all plant tissues, except pollen (Lindner *et al.*, 2012). In addition, we observed that a lack of a functional FER, but not ANX1 or ANX2, resulted in altered plant defences against *Pst* DC3000 (Figs 2 and S2) when dip inoculated with high inoculum concentration [1×10^8 colony-forming units (CFU)/mL]. However, in a different experimental set-up (syringe infiltration with 5×10^4 CFU/mL), Mang *et al.* (2017) observed that *anx1–2* and *anx2*-2 leaves can support smaller bacterial populations than Col-0 leaves. Moreover, ANX1 may act as a negative regulator of immunity by interfering with FLS2–BAK1 formation under flagellin elicitation (Mang *et al.*, 2017). These recent studies indicate that other members of CrRLK1L could also be involved in plant immune responses.

Previously, the FER mutation in *fer-5* has been shown to cause reduction in shoot size, defects in root hairs, reduction in signalling response to auxin, partial insensitivity to RALF and hypersensitivity to ABA in relation to wild-type plants (Duan *et al.*, 2010; Haruta *et al.*, 2014; Yu *et al.*, 2012). However, this is the first study to report responses to pathogen infection in the *fer-5* mutant background. We observed altered stomatal and apoplastic immune responses in *fer-5* plants after inoculation with *Pst* DC3000, such as smaller stomatal aperture and an absence of stomatal re-opening in response to this bacterium (Fig. 2). Seedlings of another FER mutant allele, named as *fer*, also exhibit smaller stomatal aperture in addition to higher accumulation of ROS (Keinath *et al.*, 2010). Increased stomatal closure in response to ABA was observed in the *fer-4* mutant allele, and was caused, at least in part, by the higher accumulation of ROS in guard cells (Yu *et al.*, 2012). Thus, it is possible that *fer-5* guard cells also accumulate high levels of ROS, and this may contribute to the constitutively smaller stomatal aperture in this mutant.

In addition, *fer-5* showed an increased resistance to *Pst* DC3000 (Fig. 2). Keinath *et al.* (2010) also observed that the FER mutation (*fer*) results in increased resistance to the *Pst* DC3000 ΔavrPtoΔavrPtoB bacterial strain, in relation to the wild-type plant. These authors attributed this phenomenon, at least in part, to the enhanced *fer* mutant cell death response that could limit bacterial proliferation (Keinath *et al.*, 2010). Moreover, this same FER mutant (*fer*) shows enhanced resistance to powdery mildew fungus infection (Kessler *et al.*, 2010). As the fungal invasion of plant cells and pollen tube perception share some common features, it has been suggested that a functional FER probably enables fungal growth and plant colonization (Kessler *et al.*, 2010). Lack of a functional FER in the *fer-4* mutant plant increases resistance to another fungus, *F. oxysporum*, in which the RALF-like peptide produced by the fungus targets FER to suppress host immunity (Masachis *et al.*, 2016). Altogether, these studies highlight the importance of FER during plant–pathogen interactions, in which FER-mediated suppression of plant immunity is a common outcome with distinct pathogens.

Previously, COK-4 has been described as a possible negative regulator of immunity in beans (Oblessuc *et al.*, 2015). In this study, we observed that COK-4 restores stomatal re-opening and leaf susceptibility in response to *Pst* DC3000 in the Arabidopsis line *fer-5* expressing this common bean kinase (Fig. 4). *Pst* DC3000 produces the phytotoxin coronatine which can promote bacterial entrance into the leaf apoplast by inhibiting stomatal closure and inducing stomatal opening (Melotto *et al.*, 2006; Panchal *et al.*, 2016a). In addition, *Pst* DC3000 effectors, such as HopX1, HopF2 and HopM1, can prevent stomatal defence and/or induce stomatal re-opening (Gimenez-Ibanez *et al.*, 2014; Hurley *et al.*, 2014; Lozano-Durán *et al.*, 2014, Melotto *et al.*, 2017). Therefore, FER of Arabidopsis and COK-4 of beans could play a role in coronatine and/or effector signalling responses to promote disease. This hypothesis is further supported by the absence of chlorosis in *fer-5* leaves inoculated with *Pst* DC3000 (Figs 2 and 4), a well-characterized symptom in response to coronatine (Melotto *et al.*, 2006). Further studies on this issue would greatly assist the understanding of COK-4 and FER function in the stomatal re-opening pathway and disease progression.

Interestingly, Col-0/*COK-4* lines support higher bacterial populations than do those of Col-0/*GFP*. This finding suggests that *COK-4* expression may have an additive dosage effect on FER-mediated regulation of plant immunity in response to *Pst* DC3000. Notably, the common bean genome has many copies of the *COK-4* gene that are highly similar, but not identical, to each other (Oblessuc *et al.*, 2015). Therefore, it is possible that the encoded COK-4 proteins work together to establish specific levels of disease reaction in different bean genotypes. This hypothesis deserves careful testing as FER, and probably COK-4, may play a role in plant–pathogen interactions, acting as negative regulators of plant immunity.

High susceptibility to a coronatine-deficient strain of *Pst* D3000 (COR^-) has been observed in *fer-2* and *fer-4* knockout mutants (Stegmann *et al.*, 2017), suggesting that FER could also promote plant immunity. FER is rapidly phosphorylated in the presence of flg22 (Benschop *et al.*, 2007) and facilitates the formation of the FLS2–BAK1 complex at the cell membrane, thereby enabling the signal transduction that induces immune responses in the plant (Chinchilla *et al.*, 2007; Stegmann *et al.*, 2017). In

addition, FER is a receptor of the small hormone peptide RALF, and RALF23–FER interaction inhibits the FER scaffold-mediated formation of the FLS2–BAK1 complex. Therefore, FER can participate in both negative and positive regulation of plant innate immunity, depending on the perception of the hormone RALF23 (Stegmann *et al.*, 2017). This highlights the importance of FER, and its malectin ectodomain, in the crosstalk between different signals in the plant. One cannot exclude that *fer-5* may be a dominant activating allele, unlike the loss-of-function alleles *fer-2* and *fer-4*. The *fer-5* allele expresses the malectin domain, but not the kinase domain (Fig. S4), whereas *fer-2* and *fer-4* are complete knockout mutants (Deslauriers and Larsen, 2010; Duan *et al.*, 2010). Recently, this phenomenon has been established for a mutant allele of another member of the CrRLK1L family, THESEUS1 (THE1). Similar to *fer-5*, the mutant *the1–4* also expresses the malectin domain, but not the kinase domain, of THE1 (Merz *et al.*, 2017). Possibly, *fer-5* may possess a functional malectin domain that can perceive the extracellular environment and associate with signal transmitting partners in a stronger manner, because of the lack of the kinase domain, resulting in a dominant phenotype. This putative gain-of-function hypothesis is yet to be tested, and will probably depend on whether FER is the transducing element or whether it requires partners to transduce the perceived signal.

FER is required for plant responses to different hormones involved in the control of growth and development (Li *et al.*, 2016). Similar to other members of the family, FER has been described as a modulator of plant development and is fundamental to cell growth (Deslauriers and Larsen, 2010; Duan *et al.*, 2010; Guo *et al.*, 2009; Haruta *et al.*, 2014; Yu *et al.*, 2012). For instance, *fer-2* seedlings are hyposensitive to the hormone BR and hypersensitive to ethylene, resulting in a small hypocotyl relative to wild-type plants (Deslauriers and Larsen, 2010). BR signalling also regulates guard cell development by inhibiting stomatal formation in leaves (Zhu *et al.*, 2013). Interestingly, we observed a reduction in stomatal aperture, guard cell complex size and guard cell length in *fer-5* leaves (Fig. 5), suggesting that FER may play a role in this hormonal control of stomatal development. In addition, *COK-4* expression partially complements these guard cell developmental defects of *fer-5*, indicating that COK-4 could be required for this process in beans. Therefore, FER and COK-4 probably act in the same signalling pathways that enable guard cell development and stomatal movement.

FER can also work in the crosstalk between ABA and auxin, evidenced by the observation that *fer-4* and *fer-5* mutants are hypersensitive to ABA and hyposensitive to auxin, resulting in the repression of shoot growth (Yu *et al.*, 2012). We also observed a reduction in *fer-5* shoot growth and other growth and developmental traits (Fig. 6). Notably, *COK-4* expression totally or partially rescued *fer-5* growth and developmental defects. Interestingly, the expression of *COK-4* in Col-0 resulted in increased biomass (Fig. 6). Thus, the number of *COK-4* copies expressed in the genome may result in distinct biomass accumulation patterns in beans.

FER may be involved in specific cell-type responses (Li *et al.*, 2015; Liao *et al.*, 2017), either as a result of the differential cell-type expression pattern of its potentially 30 RALF-like ligands (Haruta *et al.*, 2014; Stegmann *et al.*, 2017), or because of its opposite roles in ROS production in roots relative to guard cells (Yu *et al.*, 2012). Although shoot growth and defence responses were enhanced in the presence of the COK-4 protein in Col-0 plants (Figs 4 and 6), Col-0 plants with or without COK-4 were indistinguishable with regard to guard cell development, stomatal movement, days to bolting and seed weight (Figs 5 and 6). This suggests that COK-4 plays specific roles depending on the cell type, as previously hypothesized for FER. The putative kinase COK-4 is a single domain protein, whereas FER has two functional domains: an extracellular malectin domain and an intracellular kinase domain (Li *et al.*, 2016). Although it is unknown whether *fer-5* has a functional malectin domain, previous studies have shown that *fer-5* has a milder defective phenotype when compared with *fer-4*, a FER mutant allele that lacks the expression of both protein domains (Duan *et al.*, 2010; Haruta *et al.*, 2014; Yu *et al.*, 2012). Therefore, it is plausible to consider that COK-4 requires the extracellular domain of FER to be fully functional. If so, COK-4-mediated signalling responses in guard cells and reproductive tissues could be limited by the similar FER–malectin expression pattern in both Col-0 and Col-0/*COK-4* plants. However, if COK-4 does not require a FER–malectin domain to be functional in these cell types, the additive effect of *COK-4* expression in the Col-0 background could be limited by other molecular partners that have the same expression levels in both Col-0 and Col-0/*COK-4* genotypes. In this scenario, it is also possible that COK-4 may complement the function of the kinase domain of other CrRLK1L family members, as their kinase domains are functionally equivalent (Kessler *et al.*, 2014). Moreover, a third hypothesis can be considered, in which the COK-4 dosage is important in these cell types, and the expression of multiple copies of *COK-4* is necessary to fully complement the *fer-5* defects and enhance Col-0 guard cell movement and development, as well as plant reproduction.

Our study provides evidence that the common bean COK-4 acts in the same signalling pathway as the FER kinase in Arabidopsis, in which COK-4 and the FER kinase domain are required for the regulation of both shoot growth/development and plant immunity (Fig. 7). Plant growth and defence share common signalling components (Huot *et al.*, 2014; Züst and Agrawal, 2017). One of these components may be FER or COK-4 which could function as a hub for the various plant responses to distinct environmental challenges to improve plant fitness. Continued studies on both FER and COK-4 are necessary to pinpoint the steps

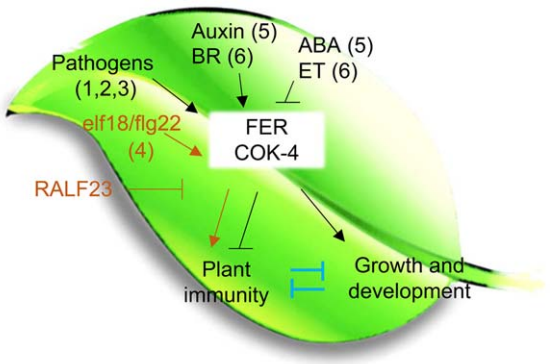

Fig. 7 Working model for the possible roles of COK-4 in the crosstalk between different signals in the control of plant shoot growth/development and immunity. The model is based on our results and previously published data: (1) Keinath *et al.* (2010); (2) Kessler *et al.* (2010); (3) Masachis *et al.* (2016); (4) Stegmann *et al.* (2017); (5) Yu *et al.* (2012); (6) Deslaurier and Larsen (2010). Orange arrows and bars indicate an alternative pathway for FERONIA (FER) function in immunity (Stegmann *et al.*, 2017). Blue bars in the model indicate the possible existence of negative crossregulation of plant immunity and growth that is independent of FER/COK-4. Arrows indicate positive regulation and bars indicate negative regulation. ABA, abscisic acid; BR, brassinosteroid; ET, ethylene; RALF, rapid alkalinization factor.

in the molecular pathway(s) in which these proteins are involved during plant–pathogen interactions and growth responses.

EXPERIMENTAL PROCEDURES

In silico analyses

The phylogenetic tree was constructed using the top 40 unique protein kinases of Arabidopsis (Table S1, see Supporting Information) with significant alignment (threshold E-value $\leq 3 \times 10^{-33}$) with the predicted COK-4 protein from the common bean line SEL 1308 [National Center for Biotechnology Information (NCBI) accession number AAF98554; Melotto and Kelly, 2001]. The Position-Specific Iterated BLAST (PSI-BLAST) program was used with the *Arabidopsis thaliana* database as query (Altschul *et al.*, 1997, 2005). The phylogenetic tree was obtained using only the kinase domain of each protein with the maximum parsimony method from MAFFT software (Katoh and Standley, 2013). The nodes were confirmed by 1000 bootstraps.

The 3D protein models for FER and COK-4 were obtained using SWISS-MODEL software (Biasini *et al.*, 2014). Both whole proteins were used for target–template alignment search with BLAST and HHBlits (Altschul *et al.*, 1997, 2005; Remmert *et al.*, 2012) against the SWISS-MODEL template library. As a 3D structure is not available for the FER protein, the Pto protein kinase crystal structure (library id 2qkw.1.B; Xing *et al.*, 2007) was used as a template to obtain the 3D models. Amongst the crystal protein structures available at the SWISS-MODEL database, Pto has the highest sequence identity with both FER (58.97%) and COK-4 (45.58%) proteins. The alignment between both protein models, COK-4 and FER, was obtained using CCP4G v.2.10.6 software (McNicholas *et al.*, 2011).

The amino acid sequence alignment was obtained using BioEdit software v.7.2.5 with the two sequence pairwise alignment method, allowing the ends to slide, or the ClustalW multiple alignment tool (Hall, 1999). The phosphorylation sites of FER and COK-4 were predicted using PhosPhAt (Durek *et al.*, 2010) and NetPhos 3.1 (Blom *et al.*, 1999) software, respectively.

ANX1, *ANX2* and *FER* expression in different Arabidopsis tissues was obtained using the developmental map from Arabidopsis eFBrowser software (http://bar.utoronto.ca; Winter *et al.*, 2007). The expression of FER during Arabidopsis guard cell development was obtained using the Arabidopsis eFBrowser and data from Adrian *et al.* (2015).

Plant material

Arabidopsis thaliana (L. Heyhn.) wild-type Columbia [Col-0, Arabidopsis Biological Resource Center (ABRC) stock CS60000], the mutant *fer-5* (ABRC stock SALK_029056c) and the Col-0 and *fer-5* lines expressing *COK-4* were sown in a 1 : 1 (v/v) mixture of growing medium (Redi-earth plug and seedling mix, Sun Gro, Sacramento, CA, USA) and perlite. Plants were kept at 4 °C for 2 days for seed stratification, and transferred to a controlled environmental chamber set at 22 °C, 60% ± 5% relative humidity and 12-h photoperiod under a light intensity of 100 μmol/m^2/s.

The *fer-5* mutant has a T-DNA insertion in the region that encodes the kinase domain at the end of its single exon. Thus, the malectin domain is expressed in this mutant, but the kinase domain is not (Fig. S4; Duan *et al.*, 2010).

To express COK-4 in Col-0 and *fer-5* plants, the *COK-4* transcript was amplified from the common bean line G2333 using the primers listed in Table S2 (see Supporting Information). G2333 is the parental line of the breeding line SEL1308 that contains the *Co-4*^{2} locus (Melotto and Kelly, 2001). *COK-4* was cloned into the pB7WGF2 vector under the control of the *Cauliflower mosaic virus* (CaMV) 35S promoter (Karimi *et al.*, 2002) to make the construct p35S-*GFP*::*COK-4*. This construct was transformed into the *Agrobacterium tumefaciens* strain C58C1 by the freeze–thaw method (Chen *et al.*, 1994), which was used to transform Col-0 and *fer*-5 plants employing the floral dip method (Clough and Bent, 1998). Col-0 plants and *fer-5* were also transformed with pB7WGF2 empty vector as controls. Transgenic lines were selected with BASTA (0.0114% glufosinate ammonium; Bayer®, Leverkusen, Germany) supplemented with 0.005% of Silwet L-77 (Lehle Seeds, Round Rock, TX, USA). The expected transgene size was confirmed with western blotting of *N. benthamiana* leaves transiently expressing either *GFP* or *GFP*::*COK-4* protein, as described below.

Gene expression analysis

To assess the gene expression of both the malectin and kinase domains from FER in wild-type Col-0 plants and the *fer-5* mutant, leaves of each genotype were ground without any treatment. Total RNA was extracted using an RNeasy mini kit (Qiagen, Hilden, Germany) with in-column DNAse treatment, according to the manufacturer's instructions. RNA was synthesized to cDNA using the Takara RNA PCR kit (AMV) (Clontech, Mountain View, CA, USA). End-point reverse transcription-polymerase chain reaction (RT-PCR) (25 μL) was performed with 1 U DNA polymerase Gotaq® (Promega, Madison, WI, USA), 1 × enzyme buffer, 1.5 mM

$MgCl_2$, 200 μM deoxynucleoside triphosphate (dNTP), 1 μL (50 ng) of cDNA template and 200 nm of reverse and forward domain-specific primers (Table S2). Reactions were carried out using the following cycling parameters: one cycle at 95 °C for 5 min, 40 cycles at 95 °C for 30 s, 60 °C for 30 s and 72 °C for 30 s, and a final extension at 72 °C for 10 min. Gene expression levels were normalized based on the expression of the housekeeping gene *ACT2* (At3g18780; Table S2). Amplicons were visualized after gel electrophoresis using the UV light on a C300 imaging system (Azure Biosystems, Dublin, CA, USA).

Protein transient expression assay

Single colonies of *A. tumefaciens* strain C58C1 containing p35S-*GFP*::*COK-4* or p35S-*GFP* construct cloned into the binary vector pB7WGF2 were selected and cultured overnight at 28 °C in Luria-Bertani (LB) medium containing 100 μg/mL rifampicin, 10 μg/mL tetracycline and 100 μg/mL spectinomycin. *Agrobacterium* cells were harvested from overnight cultures, washed in infiltration buffer [10 mM 2-(*N*-morpholino)ethanesulfonic acid (MES), pH 5.8, 10 mM $MgCl_2$, 0.2% sucrose, 300 μM acetosyringone] and suspended to an optical density at 600 nm (OD_{600}) = 0.2 also in infiltration buffer. After 3 h of incubation in the dark, cultures were syringe infiltrated into mature leaf tissue of *N. benthamiana*. Infiltrated plants were returned to previous growing conditions (12-h photoperiod and 25 °C) and fluorescence was observed by microscopy at 2–3 days after inoculation. In addition, the transgene was detected using western blotting as described by Thines *et al.* (2007), with modifications. Briefly, after the extraction of soluble protein from leaves using protein buffer [100 mM dithiothreitol (DTT), 2% sodium dodecylsulfate (SDS), 50 mM tris(hydroxymethyl)aminomethane (Tris)-HCl, pH 6.8, 10% glycerol], samples were run on a Mini-protein® TGX Stain-Free sodium dodecylsulfate-polyacrylamide gel electrophoresis (SDS-PAGE) gel (BioRad, Hercules, CA, USA). After electrophoresis, proteins were transferred to a polyvinylidene difluoride (PVDF) membrane (PVDF-Plus, Micron Separations Inc., Westborough, MA, USA). Protein transfer was performed in a Trans-Bolt SD Cell (BioRad) set for 15 V for 20 min. The membrane was then incubated with the primary antibody (anti-GFP, 1 : 50 000; Life Technologies, Carlsbad, CA, USA), overnight at 4 °C, on an orbital shaker (75 rpm). The secondary antibody (anti-Rabbit IgG, 1 : 150 000; Life Technologies) was incubated for 2 h at room temperature. Membrane development was performed using chemiluminescent substrates (SuperSignal West Femto trial kit, Thermo Scientific, Rockford, IL, USA), detected with the CHEMI tool of a C300 imaging system (Azure Biosystems).

Microscopy

BASTA-resistant plants and control non-transformed plants were analysed for the presence of the GFP signal with a Nikon Eclipse 80i fluorescent microscope equipped with a Fluorescein IsoThioCyanate (FITC) filter (475–495 nm), Differential Interference Contrast (DIC) and long-distance objectives, using NIS Elements Imaging software (Nikon Corporations, Shinagawa-ku, Tokyo, Japan).

Pathogenesis assay

Pathogenesis assay was conducted using *Pst* DC3000, as described previously (Jacob *et al.*, 2017; Katagiri *et al.*, 2002). Briefly, plants were dip inoculated with 1×10^8 CFU/mL or vacuum infiltrated with 1×10^6 CFU/mL of bacterial suspension containing 0.03% or 0.004% of Silwet L-77 (Lehle Seeds), respectively. The bacterial population in the leaf apoplast was determined on days 1 and 3 after infection using a serial dilution-based method.

Stomatal bioassay

The stomatal response to the bacterium was assessed in 4–5-week-old plants as described previously (Montano and Melotto, 2017). As differences in stomatal movements could be attributed to developmental defects in mutants and transgenic plants, stomatal complex dimensions were also measured as follows: stomatal aperture width (*A*), stomatal complex width (*W*), guard cell pair size ($W - A$), length of the stomatal complex (*L*) and size of the stomatal complex ($W \times L$), as described by Panchal *et al.* (2016b). The stomatal measurements were taken using non-treated mature leaves at 3 h after the lights had been turned on in the morning.

Plant growth and developmental evaluations

Plant growth and developmental phenotypes were evaluated using several parameters. First, the fresh and dry weights of 35-day-old plant rosettes were measured following the procedure described by Abe *et al.* (2003). Briefly, rosettes were collected and immediately weighed for fresh weight, and the same rosettes were placed at 70 °C for 72 h to obtain the dry weight. Second, the number of true leaves produced by the apical meristem was recorded on bolted plants (around 35-day-old plants), following the description by Pouteau *et al.* (2004). Third, the bolting time was determined as the number of days from sowing to the elongation of the first floral stem at 0.1 cm height (Pouteau *et al.*, 2004). Fourth, the seed weight was measured by collecting and weighing the seeds produced by each plant grown under standard conditions, as described above. Fifth, the days to seedling emergence were determined from the time of sowing to the germination of seedlings, i.e. when the cotyledons were visible. All measurements were obtained from three biological replicates ($n = 5–51$).

Statistical analyses

Statistical analyses were performed using Student's *t*-test or analysis of variance (ANOVA) followed by Scott–Knott's test at 5% probability using InfoStat statistical software (Di Rienzo *et al.*, 2014). All experiments were performed at least three times with similar results, where the data points represent the mean ± standard error (SE).

ACKNOWLEDGEMENTS

We thank Dr Nathan Pumplin for helpful discussions on this research and the Brazilian Funding Agency CAPES (Coordenação de Aperfeiçoamento de Pessoal de Nível Superior) for a scholarship to RFA (award number BEX 3517/15-2). The authors declare no conflicts of interest.

AUTHOR CONTRIBUTIONS

PRO and MM conceived the project and designed all the research. RFA and PRO performed the experiments. RFA, PRO and MM

analysed the data. MCGV and MM provided the materials. RFA, PRO and MM wrote the article.

REFERENCES

Abe, H., Urao, T., Ito, T., Seki, M., Shinozaki, K. and Yamaguchi-Shinozaki, K. (2003) Arabidopsis AtMYC2 (bHLH) and AtMYB2 (MYB) function as transcriptional activators in abscisic acid signaling. *Plant Cell*, **15**, 63–78.

Adrian, J., Chang, J., Ballenger, C.E., Bargmann, B.O., Alassimone, J., Davies, K.A., Lau, O.S., Matos, J.L., Hachez, C., Lanctot, A., Vatén, A., Birnbaum, K.D. and Bergmann, D.C. (2015) Transcriptome dynamics of the stomatal lineage: birth, amplification, and termination of a self-renewing population. *Dev. Cell*, **33**, 107–118.

Altschul, S.F., Madden, T.L., Schaffer, A.A., Zhang, J., Zhang, Z., Miller, W. and Lipman, D.J. (1997) Gapped BLAST and PSI-BLAST: a new generation of protein database search programs. *Nucleic Acids Res.* **25**, 3389–3402.

Altschul, S.F., Wootton, J.C., Gertz, E.M., Agarwala, R., Morgulis, A., Schaffer, A.A. and Yu, Y.K. (2005) Protein database searches using compositionally adjusted substitution matrices. *FEBS J.* **272**, 5101–5109.

Belkhadir, Y., Yang, L., Hetzel, J., Dangl, J.L. and Chory, J. (2014) The growth–defense pivot: crisis management in plants mediated by LRR-RK surface receptors. *Trends Biochem. Sci.* **39**, 447–456.

Benschop, J.J., Mohammed, S., O'Flaherty, M., Heck, A.J.R., Slijper, M. and Menke, F.L.H. (2007) Quantitative phosphoproteomics of early elicitor signaling in Arabidopsis. *Mol. Cell. Proteomics*, **6**, 1198–1214.

Biasini, M., Bienert, S., Waterhouse, A., Arnold, K., Studer, G., Schmidt, T., Kiefer, F., Gallo, C.T., Bertoni, M., Bordoli, L. and Schwede, T. (2014) SWISS-MODEL: modelling protein tertiary and quaternary structure using evolutionary information. *Nucleic Acids Res.* **42**, 252–258.

Blom, N., Gammeltoft, S. and Brunak, S. (1999) Sequence- and structure-based prediction of eukaryotic protein phosphorylation sites. *J. Mol. Biol.* **5**, 1351–1362.

Boisson-Dernier, A., Roy, S., Kritsas, K., Grobei, M. A., Jaciubek, M., Schroeder, J.I. and Grossniklaus, U. (2009) Disruption of the pollen-expressed FERONIA homologs ANXUR1 and ANXUR2 triggers pollen tube discharge. *Development*, **136**, 3279–3288.

Campos, M.L., Yoshida, Y., Major, I.T., Ferreira, D.O., Weraduwage, S.M., Froehlich, J.E., Johnson, B.F., Kramer, D.M., Jander, G., Sharkey, T.D. and Howe, G.A. (2016) Rewiring of jasmonate and phytochrome B signalling uncouples plant growth–defense tradeoffs. *Nat. Commun.* **7**, 12 570.

Chen, D.H., Leu, J.C. and Huang, T.C. (1994) Transport and hydrolysis of urea in a reactor–separator combining an anion-exchange membrane and immobilized urease. *J. Chem. Technol. Biotechnol.* **61**, 351–357.

Chinchilla, D., Zipfel, C., Robatzek, S., Kemmerling, B., Nürnberger, T., Jones, J.D., Felix, G. and Boller, T. (2007) A flagellin-induced complex of the receptor FLS2 and BAK1 initiates plant defence. *Nature*, **448**, 497.

Clough, S.J. and Bent, A.F. (1998) Floral dip: a simplified method for *Agrobacterium*-mediated transformation of *Arabidopsis thaliana*. *Plant J.* **16**, 735–743.

Deslauriers, S.D. and Larsen, P.B. (2010) FERONIA is a key modulator of brassinosteroid and ethylene responsiveness in Arabidopsis hypocotyls. *Mol. Plant.* **3**, 626–640.

Di Rienzo, J.A., Casanoves, F., Balzarini, M.G., Gonzalez, L., Tablada, M. and Robledo, C.W. (2014) *InfoStat versión 2014*. Argentina: InfoStat Group, Facultad de Ciencias Agropecuarias, Universidad Nacioal de Córdoba. Available at http://www.infostat.com.ar [accessed 23 January 2018].

Duan, Q., Kita, D., Li, C., Cheung, A.Y. and Wu, H.M. (2010) FERONIA receptor-like kinase regulates RHO GTPase signaling of root hair development. *Proc. Natl. Acad. Sci. USA*, **107**, 17 821–17 826.

Durek, P., Schmidt, R., Heazlewood, J.L., Jones, A., Maclean, D., Nagel, A., Kersten, B. and Schulze, W.X. (2010) PhosPhAt: the *Arabidopsis thaliana* phosphorylation site database. An update. *Nucleic Acids Res.* **38**, 828–834.

Escobar-Restrepo, J.M., Huck, N., Kessler, S., Gagliardini, V., Gheyselinck, J., Yang, W.C. and Grossniklaus, U. (2007) The FERONIA receptor-like kinase mediates male–female interactions during pollen tube reception. *Science*, **317**, 656–660.

Gimenez-Ibanez, S., Boter, M., Fernández-Barbero, G., Chini, A., Rathjen, J.P. and Solano, R. (2014) The bacterial effector HopX1 targets JAZ transcriptional repressors to activate jasmonate signaling and promote infection in Arabidopsis. *PLoS Biol.* **12**, e1001792.

Guo, H., Li, L., Ye, H., Yu, X., Algreen, A. and Yin, Y. (2009) Three related receptor-like kinases are required for optimal cell elongation in *Arabidopsis thaliana*. *Proc. Natl. Acad. Sci. USA*, **106**, 7648–7653.

Hall, T.A. (1999) BioEdit: a user-friendly biological sequence alignment editor and analysis program for Windows 95/98/NT. *Nucleic Acids Symp. Ser.* **41**, 95–98.

Haruta, M., Sabat, G., Stecker, K., Minkoff, B.B. and Sussman, M.R. (2014) A peptide hormone and its receptor protein kinase regulate plant cell expansion. *Science*, **343**, 408–411.

Huot, B., Yao, J., Montgomery, B.L. and He, S.Y. (2014) Growth–defense tradeoffs in plants: a balancing act to optimize fitness. *Mol. Plant.* **7**, 1267–1287.

Hurley, B., Lee, D., Mott, A., Wilton, M., Liu, J., Liu, Y.C., Angers, S., Coaker, G., Guttman, D.S. and Desveaux, D. (2014) The *Pseudomonas syringae* type III effector HopF2 suppresses Arabidopsis stomatal immunity. *PLoS One*, **9**, 1–20.

Jacob, C., Panchal, S. and Melotto, M. (2017) Surface inoculation and quantification of *Pseudomonas syringae* population in the Arabidopsis leaf apoplast. *Bio. Protoc.* **7**, e2167.

Karimi, M., Inzé, D. and Depicker, A. (2002) GATEWAY vectors for *Agrobacterium*-mediated plant transformation. *Trends Plant Sci.* **7**, 193–195.

Katagiri, F., Thilmony, R. and He, S.Y. (2002) *The Arabidopsis thaliana–Pseudomonas syringae Interaction*. The Arabidopsis Book. American Society of Plant Biologists. Available at http://www.aspb.org/publications/arabidopsis [accessed 18 June 2015].

Katoh, K. and Standley, D.M. (2013) MAFFT multiple sequence alignment software version 7: improvements in performance and usability. *Mol. Biol. Evol.* **30**, 772–780.

Keinath, N.F., Kierszniowska, S., Lorek, J., Bourdais, G., Kessler, S.A., Shimosato-Asano, H., Grossniklaus, U., Schulze, W.X., Robatzek, S. and Panstruga, R. (2010) PAMP (pathogen-associated molecular pattern)-induced changes in plasma membrane compartmentalization reveal novel components of plant immunity. *J. Biol. Chem.* **285**, 39 140–39 149.

Kessler, S.A., Shimosato-Asano, H., Keinath, N.F., Wuest, S.E., Ingram, G., Panstruga, R. and Grossniklaus, U. (2010) Conserved molecular components for pollen tube reception and fungal invasion. *Science*, **330**, 968–971.

Kessler, S.A., Lindner, H., Jones, D.S. and Grossniklaus, U. (2014) Functional analysis of related CrRLK1L receptor-like kinases in pollen tube reception. *EMBO Rep.* **16**, 107–115.

Li, C., Yeh, F.-L., Cheung, A.Y., Duan, Q., Kita, D., Liu, M.-C., Maman, J., Luu, E.J., Wu, B.W., Gates, L. and Jalal, M. (2015) Glycosylphosphatidylinositol-anchored proteins as chaperones and co-receptors for FERONIA receptor kinase signaling in Arabidopsis. *Elife*, **4**, e06587.

Li, C., Wu, H.M. and Cheung, A.Y. (2016) FERONIA and her pals: functions and mechanisms. *Plant Physiol.* **171**, 2379–2392.

Liao, H., Tang, R., Zhang, X., Luan, S. and Yu, F. (2017) FERONIA receptor kinase at the crossroads of hormone signaling and stress responses. *Plant Cell Physiol.* **58**, 1143–1150.

Lindner, H., Müller, L.M., Boisson-Dernier, A. and Grossniklaus, U. (2012) CrRLK1L receptor-like kinases: not just another brick in the wall. *Curr. Opin. Plant Biol.* **15**, 659–669.

Lozano-Durán, R. and Zipfel, C. (2015) Trade-off between growth and immunity: role of brassinosteroids. *Trends Plant Sci.* **20**, 12–19.

Lozano-Durán, R., Bourdais, G., He, S.Y. and Robatzek, S. (2014) The bacterial effector HopM1 suppresses PAMP-triggered oxidative burst and stomatal immunity. *New Phytol.* **202**, 259–269.

Mang, H., Feng, B., Hu, Z., Boisson-Dernier, A., Franck, C., Meng, X., Huang, Y., Zhou, J., Xu, G., Wang, T., Shan, L. and He, P. (2017) Differential regulation of two-tiered plant immunity and sexual reproduction by ANXUR receptor-like kinases. *Plant Cell*, **1**, tpc.00464.

Masachis, S., Segorbe, D., Turrà, D., Leon-Ruiz, M., Fürst, U., El-Ghalid, M., Leonard, G., López-Berges, M.S., Richards, T.A., Felix, G. and Di Pietro, A. (2016) A fungal pathogen secretes plant alkalinizing peptides to increase infection. *Nat. Microbiol.* **1**, 16 043.

McNicholas, S., Potterton, E., Wilson, K.S. and Noble, M.E.M. (2011) Presenting your structures: the CCP4mg molecular-graphics software. *Acta Crystallogr. D: Biol. Crystallogr.* **67**, 386–394.

Melotto, M. and Kelly, J.D. (2001) Fine mapping of the *Co-4* locus of common bean reveals a resistance gene candidate, COK-4, that encodes for a protein kinase. *Theor. Appl. Genet.* **103**, 508–517.

Melotto, M., Coelho, M.F., Pedrosa-Harand, A., Kelly, J.D. and Camargo, L.E.A. (2004) The anthracnose resistance locus *Co-4* of common bean is located on

chromosome 3 and contains putative disease resistance-related genes. *Theor. Appl. Genet.* **109**, 690–699.
Melotto, M., Underwood, W., Koczan, J., Nomura, K. and He, S.Y. (2006) Plant stomata function in innate immunity against bacterial invasion. *Cell*, **126**, 969–980.
Melotto, M., Zhang, L., Oblessuc, P.R. and He, S.Y. (2017) Stomatal defense a decade later. *Plant Physiol.* **174**, 561–571.
Merz, D., Richter, J., Gonneau, M., Sanchez-Rodriguez, C., Eder, T., Sormani, R., Martin, M., Hématy, K., Höfte, H. and Hauser, M.T. (2017) T-DNA alleles of the receptor kinase THESEUS1 with opposing effects on cell wall integrity signaling. *J. Exp. Bot.* **68**, 4583–4593.
Miyazaki, S., Murata, T., Sakurai-Ozato, N., Kubo, M., Demura, T., Fukuda, H. and Hasebe, M. (2009) ANXUR1 and 2, sister genes to FERONIA/SIRENE, are male factors for coordinated fertilization. *Curr. Biol.* **19**, 1327–1331.
Montano, J. and Melotto, M. (2017) Stomatal bioassay to characterize bacterial-stimulated PTI at the pre-invasion phase of infection. In: *Methods in Molecular Biology*, Vol. **1578** (Shan, L. and He, P., eds), pp. 233–241. Springer Protocols, Humana Press, New York.
Nissen, K.S., Willats, W.G. and Malinovsky, F.G. (2016) Understanding CrRLK1L function: cell walls and growth control. *Trends Plant Sci.* **21**, 516–527.
Oblessuc, P.R., Francisco, C. and Melotto, M. (2015) The *Co-4* locus on chromosome Pv08 contains a unique cluster of 18 COK-4 genes and is regulated by immune response in common bean. *Theor. Appl. Genet.* **128**, 1193–1208.
Panchal, S., Chitrakar, R., Thompson, B.K., Obulareddy, N., Roy, D., Hambright, W.S. and Melotto, M. (2016b) Regulation of stomatal defense by air relative humidity. *Plant Physiol.* **172**, 2021–2032.
Panchal, S., Roy, D., Chitrakar, R., Price, L., Breitbach, Z.S., Armstrong, D.W. and Melotto, M. (2016a) Coronatine facilitates *Pseudomonas syringae* infection of Arabidopsis leaves at night. *Front. Plant Sci.* **7**, 880.
Pouteau, S., Ferret, V., Gaudin, V., Lefebvre, D., Sabar, M., Zhao, G. and Prunus, F. (2004) Extensive phenotypic variation in early flowering mutants of Arabidopsis. *Plant Physiol.* **135**, 201–211.
Remmert, M., Biegert, A., Hauser, A. and Soding, J. (2012) HHblits: lightning-fast iterative protein sequence searching by HMM-HMM alignment. *Nat. Methods*, **9**, 173–175.
Stegmann, M., Monaghan, J., Smakowska-Luzan, E., Rovenich, H., Lehner, A., Holton, N., Belkhadir, Y. and Zipfel, C. (2017) The receptor kinase FER is a RALF-regulated scaffold controlling plant immune signaling. *Science*, **355**, 287–289.
Thines, B., Katsir, L., Melotto, M., Niu, Y., Mandaokar, A., Liu, G., Nomura, K., He, S.Y., Howe, G.A. and Browse, J. (2007) JAZ repressor proteins are targets of the SCF(COI1) complex during jasmonate signalling. *Nature*, **448**, 661–665.
Winter, D., Vinegar, B., Nahal, H., Ammar, R., Wilson, G.V. and Provart, N.J. (2007) An "Electronic Fluorescent Pictograph" browser for exploring and analyzing large-scale biological data sets. *PLoS One*, **2**, 718.
Xing, W., Zou, Y., Liu, Q., Liu, J., Luo, X., Huang, Q., Chen, S., Zhu, L., Bi, R., Hao, Q., Wu, J.W., Zhou, J.M. and Chai, J. (2007) The structural basis for activation of plant immunity by bacterial effector protein AvrPto. *Nature*, **449**, 243–247.
Yu, F., Qian, L., Nibau, C., Duan, Q., Kita, D., Levasseur, K., Li, X., Lu, C., Li, H., Hou, C., Li, L., Buchanan, B.B., Chen, L. and Cheung, A.Y. (2012) FERONIA receptor kinase pathway suppresses abscisic acid signaling in Arabidopsis by activating ABI2 phosphatase. *Proc. Natl. Acad. Sci. USA*, **109**, 14 693–14 698.
Zhu, J.Y., Sae-Seaw, J. and Wang, Z.Y. (2013) Brassinosteroid signalling. *Development*, **140**, 1615–1620.
Züst, T. and Agrawal, A.A. (2017) Plant chemical defense indirectly mediates aphid performance via interactions with tending ants. *Ecology*, **98**, 601–607.

SUPPORTING INFORMATION

Additional Supporting Information may be found in the online version of this article at the publisher's website:

Table S1 Top 40 genes with protein sequence similarity to COK-4 [National Center for Biotechnology Information (NCBI) accession number AAF98554] using the Position-Specific Iterated BLAST (PSI-BLAST) program and the *Arabidopsis thaliana* database (Altschul *et al.*, 1997, 2005).

Table S2 Primer names and sequences.

Fig. S1 FERONIA (FER) and COK-4 protein alignment and phosphorylation motif analyses. (A) Diagram showing the alignment between FER and COK-4 proteins determined with the two sequence pairwise alignment function of BioEdit v.7.2.5. Coding regions for the kinase, transmembrane (TM) and two malectin domains are indicated. The kinase domain residue alignment is shown below the diagram. COK-4 does not align outside of the FER kinase domain. Kinase domain motifs were identified using the National Center for Biotechnology Information (NCBI) Conserved Domain Database (CDD) and are highlighted in yellow (conserved domain cd14066: STKc_IRAK; FER, E-value $= 1.6 \times 10^{-86}$; COK-4, E-value $= 4.8 \times 10^{-58}$). Black stars indicate predicted phosphorylation sites, and red stars indicate experimentally determined phosphorylation sites in the FER protein. Shared serine (S), threonine (T) and tyrosine (Y) between COK-4 and FER are highlighted in green. The predicted transmembrane region of COK-4, determined by Melotto and Kelly (2001), is underlined, and the region identified in the predicted COK-4 three-dimensional (3D) protein model with no overlap with the FER 3D protein (see Fig. 1) is shown in bold. (B) Predicted phosphorylation sites for COK-4 and the FER kinase domain.

Fig. S2 Alignment between COK-4 (GenBank: AAF98554.1) and the kinase domain of all 40 proteins used for phylogenetic analysis [see Table S1 (Supporting Information) for PSI-BLAST results]. The alignment was obtained using the ClustalW multiple alignment tool of the BioEdit software v.7.2.5. It should be noted that COK-4 has a single kinase domain that only aligns with the kinase domain of all proteins. The COK-4 sequence is highlighted in yellow and its closest sequence (AT3G51550) is FERONIA (FER).

Fig. S3 Analyses of the Arabidopsis *FERONIA* (*FER*), *ANXUR* 1 and 2. (A–C) Diagrams depicting the developmental map of gene expression for *ANX1, ANX2* and *FER* adapted from Arabidopsis eFBrowser. (D, E) Apoplastic bacterial population in leaves of Col-0 and mutant plants after dip inoculation with 1×10^8 colony-forming units (CFU)/mL of *Pseudomonas syringae* pv. *tomato* (*Pst*) DC3000, 1 and 3 days after inoculation. Results are shown as the mean ($n = 6 \pm$ SE), and statistical significance between Col-0 and each mutant was performed using Student's *t*-test (ns, non-significant). The schematic representation below each graph shows the *ANX1* and *ANX2* gene structures adapted from TAIR (The Arabidopsis Information Resource) gene modelling. Coding regions for the kinase, transmembrane (TM) and two malectin domains are indicated, as well as the position of the T-DNA insertion present in the

SALK_016179C (*anx1-1*) and SALK_133057C (*anx2-2*) lines. The dark blue box indicates the coding domain sequences, the light blue boxes indicate the untranslated regions (UTRs) of the genes and black lines represent the intron.

Fig. S4 Arabidopsis *fer-5* mutant lacks expression of the kinase domain. (A) Reverse transcription-polymerase chain reaction (RT-PCR) amplification of the malectin and kinase encoding regions of *FERONIA* (*FER*) of Col-0 and the *fer-5* mutant. *ACT2* was used as an RNA loading control. It should be noted that *fer-5* lacks the kinase domain. (B) Schematic representation of the *FER* gene structure adapted from TAIR (The Arabidopsis Information Resource) gene modelling. Coding regions for the kinase, transmembrane (TM) and two malectin domains are indicated, as well as the position of the T-DNA insertion present in the SALK_029056C line. The dark blue box indicates the coding domain sequence, the light blue boxes indicate the untranslated regions (UTRs) of the gene and the black lines represent the intron. The arrows indicate the region in which the primers used in (A) align with the *FER* gene.

Fig. S5 (A) Transient expression in *Nicotiana benthamiana*. Western blot analysis using anti-green fluorescent protein (anti-GFP) and total proteins extracted from leaves transiently expressing the indicated construct. The number above each gel lane indicates: 1, protein standard (Bio-Rad®); 2, GFP::COK-4 protein (69.2 kDa); 3, GFP protein (26.9 kDa). Fluorescence micrographs of *N. benthamiana* leaves showing the GFP signal in cells transformed with either *GFP* (control) or a *GFP*::*COK-4* construct. BF, bright field. (B, C) Col-0 and *fer-5* have the same stomatal response to *Pseudomonas syringae* pv. *tomato* (*Pst*) DC3000 as the respective transgenic lines expressing GFP. (B) Col-0 wild-type (WT) and Col-0/*GFP* (p35S-*GFP*) and (C) *fer-5* mutant and *fer-5*/GFP (p35S-*GFP*). Plants were dip inoculated with 1×10^8 CFU/mL of *Pst* DC3000 and the stomatal aperture was assessed at 2 and 4 h post-inoculation (hpi). Results are shown as the mean ($n = 195–240 \pm$ SE), and statistical significance amongst the means, indicated by different letters above the bars, was calculated with analysis of variance (ANOVA) followed by Scott–Knott's test ($P \leq 0.05$).

Fig. S6 FERONIA (FER) affects plant growth and development. (A) Photograph of 3-week-old Col-0 and *fer-5* plants grown under the conditions described in Experimental procedures. Note the *fer-5* mutant dwarf phenotype. (B, C) Graphs showing average fresh (B) and dry (C) weights of 4–5-week-old Arabidopsis rosettes. (D) Number of leaves at maturity (4–5 weeks of age). (E) Days to bolting. (F) Seed weight ($n = 5 \pm$ SE). (G) Days to seedling emergence. Data points represent the mean ($5 < n < 51 \pm$ SE), and statistical significance was calculated by Student's *t*-test (***$p \leq 0.001$; ns, non-significant). Note that some error bars are too small and cannot be seen at the scale used in the graphs.